JACS
JOURNAL OF THE AMERICAN CHEMICAL SOCIETY
Article
pubs.acs.org/JACS

Extraordinary Stability of Naphthalenediimide Radical Ion and Its Ultra-Electron-Deficient Precursor: Strategic Role of the Phosphonium Group

Sharvan Kumar,[†,§] M. R. Ajayakumar,[†,§] Geeta Hundal,[‡,∥] and Pritam Mukhopadhyay*[,†]

[†]Supramolecular and Material Chemistry Lab, School of Physical Sciences, Jawaharlal Nehru University, New Delhi-110067, India
[‡]Department of Chemistry, X-Ray Crystallography Laboratory, Guru Nanak Dev University, Amritsar-143005, India

Supporting Information

ABSTRACT: Stabilization of radical ions and highly electron-deficient systems under ambient conditions is of great significance. A new design concept is presented that applies the multifaceted features of the phosphonium group to achieve isolation of (a) the first naphthalenediimide (NDI) radical ion [(**1a**$^{\bullet+}$)BPh_4^-] as single crystals and (b) an ultra-electron-deficient NDI [(**1a**$^{2+}$)$2BF_4^-$] having the lowest LUMO level recorded for an NDI, overwhelming the formative tetracyanoquinodimethane (**TCNQ**) molecule. Both **1a**$^{\bullet+}$ and **1a**$^{2+}$ exhibit unprecedented stability to normal workup procedures, chromatography, and anion metathesis in open air. To our knowledge, this is the first instance where radical ions stable toward chromatography have been obtained, which is a noteworthy development in the field of synthetic radical chemistry. The crucial components of thermodynamic and kinetic stabilization, namely, the nonbonded P···O interaction, hypervalency, and propeller-like shape of the phosphonium groups in **1a**$^{2+}$ and **1a**$^{\bullet+}$, were substantiated by crystallography and theoretical studies. Natural bond orbital (NBO) calculations validated the P···O contact to be an $n_O \rightarrow \sigma^*_{P-C}$ orbital interaction. Spontaneous electron transfer reactions of **1a**$^{2+}$ even in nonpolar solvents, anion−π interactions of **1a**$^{2+}$ with the naphthalene core, and panchromism of **1a**$^{\bullet+}$ are the other emergent properties. The high-yielding (~90%) in situ synthesis of **1a**$^{\bullet+}$ and the extraordinary stability fostered by the phosphonium group have the potential to turn hitherto unstable organic systems into a new genre of stable *off-the-shelf* systems.

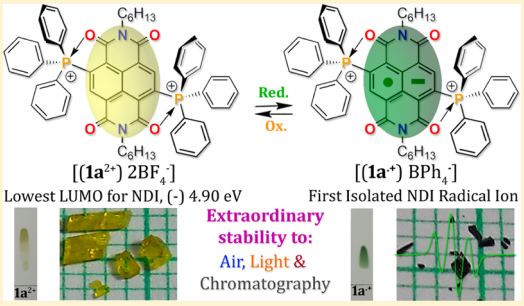

INTRODUCTION

Stabilization of organic radicals through rational design is of prime interest because of their diverse spin-based applications.[1,2] In spite of the pioneering design strategies, a radical ion that can be synthesized, purified, and crystallized under ambient conditions is still elusive. There are several classes of radical ions with fascinating optoelectronic properties that are yet to be isolated in stable form. One of the most notable among these is the class of arylenediimide-based radical ions. The other aspect with significant bearing on organic electronics[3] is the challenge of synthesizing and isolating highly electron-deficient arylenediimides (precursors to the radical anions) because of their instability under ambient conditions. We anticipated that a new design concept incorporating intramolecular nonbonded interactions should bestow additional thermodynamic stability to these systems and provide a unified solution to the above problems.

Taking a cue from the seminal Wittig reaction and organic moieties stabilized by intramolecular interactions (Figure 1),[4] we envisaged that the phosphonium group, because of its special electronic attributes (I−IV) would play a crucial role in the stabilization of the reactive naphthalenediimide (NDI) radical ion and unstable highly electron-deficient NDI systems utilizing the proximal O atoms of the imide groups (Figure 2a,b).

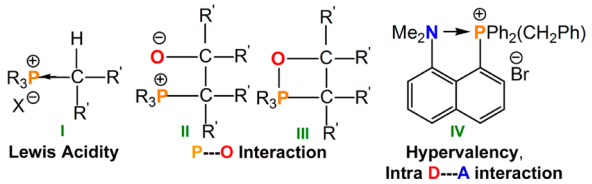

Figure 1. Diverse modes of function and stabilization driven by the phosphonium group.

In recent times, the phosphonium group's Lewis acidity, ability to undergo chelation, and structural features have been applied toward tunable π systems, anion sensing, and synthesis of liquid crystals.[5−7] However, there have been no design-based attempts employing these novel attributes to stabilize and isolate radical ions and highly electron-deficient organic systems.

NDIs have seen remarkable advances in the areas of self-assembly;[8] anion interactions, transport, and catalysis;[9,10] amine- and anion-driven electron transfer (ET) reactions;[11,12]

Received: May 16, 2014
Published: August 5, 2014

   dx.doi.org/10.1021/ja504903j | J. Am. Chem. Soc. 2014, 136, 12004−12010

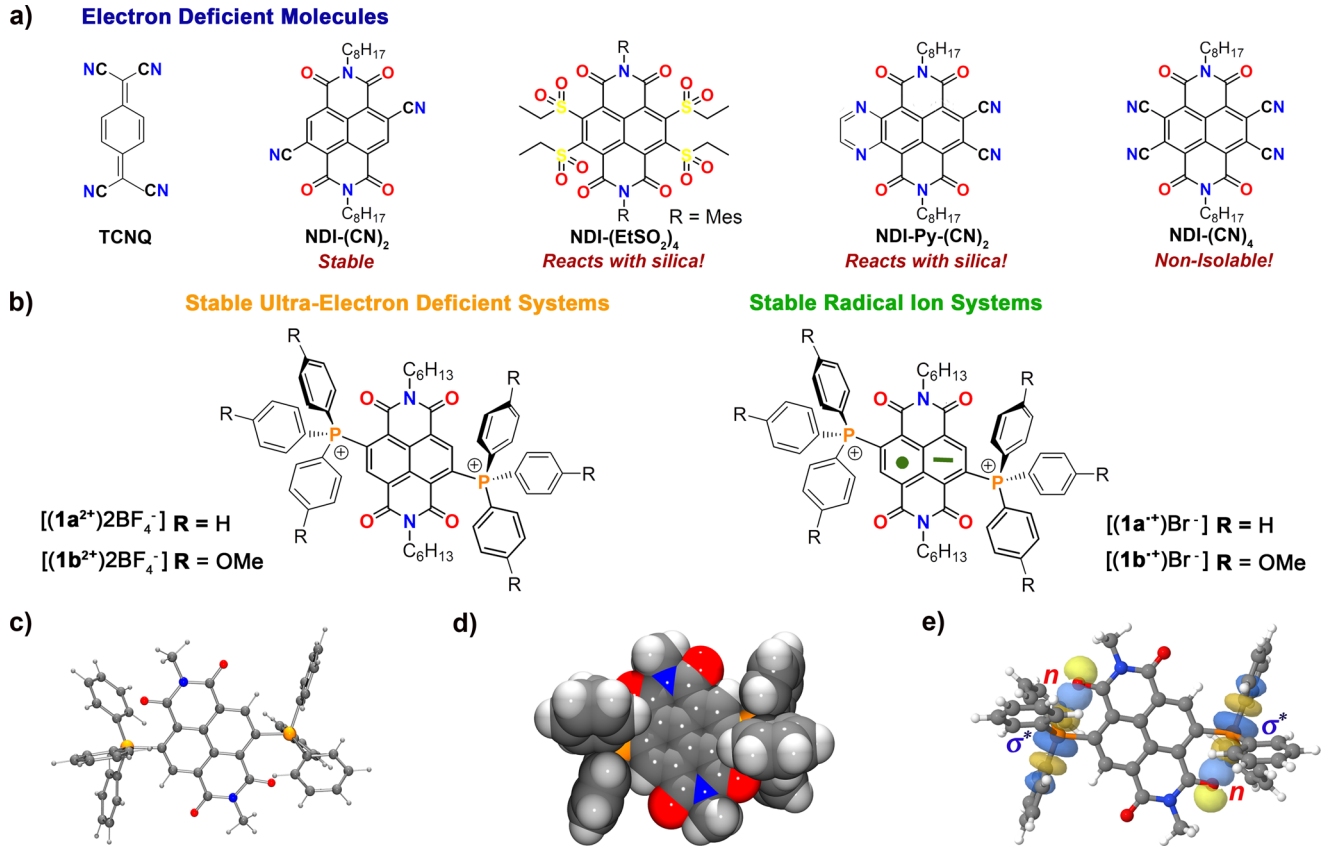

Figure 2. (a) NDI-based highly electron-deficient systems. (b) Molecular structures of ultra-electron-deficient $[(\mathbf{1a}^{2+})2BF_4^-]$ and the NDI-based radical ion $[(\mathbf{1a}^{\bullet+})Br^-]$. (c) Energy-optimized structure of $\mathbf{1a}^{2+}$. (d) Space-filling model of $\mathbf{1a}^{2+}$ depicting the propeller-like arrangement of the phosphonium group. (e) Intramolecular $n_O \rightarrow \sigma^*_{P-C}$ orbital interaction between the donor O lone pair of the imide group and the acceptor P−C σ^* orbital, as established by NBO calculations.

DNA binding;[13] and organic electronics.[14] On the other hand, after the first report of the NDI radical anion ($NDI^{\bullet-}$) way back in 1967,[15] $NDI^{\bullet-}$ species that are isolable and stable under ambient conditions have been unknown to date. $NDI^{\bullet-}$ is known to be persistent[16] in solution for up to a few days and eventually decompose into multiple products. In the absence of any rational design to isolate these reactive species, no structural data are available. The only related report has been the isolation of the radical anion of its dianhydride ($NTCDA^{\bullet-}$) by electrocrystallization.[17] However, this radical ion had an unusual stoichiometry, and its insolubility precluded its detailed characterization.

We have been interested in the study of selective ET reactions of NDIs and the application of the fascinating properties of $NDI^{\bullet-}$ species as a new class of multimodal probes.[11] In parallel, our endeavors have been directed toward enhancing the lifetimes of the NDI radical ions utilizing diverse design strategies. For example, by employing steric protection of the spin and charge and employing H-bonding units we could substantially increase the persistence of the NDI radical cations ($NDI^{\bullet+}$) as well as $NDI^{\bullet-}$ derived from core-functionalized bis(amino) NDIs.[18a] Also, extending the delocalization of the spin and charge through axial fusion of a dithiafulvalene moiety with NDI increased the lifetime of NDI-based radical ions.[18b] However, these design efforts could not bestow adequate stability to these NDI radical ions for their isolation under ambient conditions.

The other significant aspect is the instability of NDI molecules with low-lying lowest unoccupied molecular orbitals (LUMOs) (Figure 2a and Table 1).[19] For instance, in spite of the great academic and commercial interests, **NDI-(CN)$_4$**, regarded to be the strongest NDI π-acid, is yet to be obtained.[9b] In a pioneering approach, multiple sulfone groups have been incorporated to achieve the strongest NDI-based acceptor, **NDI-(EtSO$_2$)$_4$**, known as a super-π-acid.[20] However, these molecules with LUMO energies below −4.60 eV were found to be reactive toward polar solvents and unstable toward silica gel chromatography. These aspects with multidimensional implications became our prime motivation behind this ensuing research.

Table 1. LUMO Levels of Highly Electron-Deficient Systems

		E_{LUMO} (eV)	
entry	low-LUMO molecule	exptl[e]	theor
1	**TCNQ**[a]	−4.84	–
2	**NDI-(CN)$_2$**[a]	−4.53	–
3	**NDI-(EtSO$_2$)$_4$**[b]	−4.74	–
4	**NDI-Py-(CN)$_2$**[c]	−4.66	–
5	**NDI-(CN)$_4$**[d]	–	−4.82

[a]This work. [b]Reference 20. [c]Reference 19a. [d]Reference 9b. [e]The LUMO energies in entries 1 and 2 were calculated as $E_{LUMO} = [-5.1(Fc) - E_{1R}]$ eV against vacuum on the basis of CV experiments.

dx.doi.org/10.1021/ja504903j | J. Am. Chem. Soc. 2014, 136, 12004−12010

RESULTS AND DISCUSSION

Design and Synthesis. We envisaged that the phosphonium group, by virtue of its (a) Lewis acidity, (b) propensity to undergo P···O interactions, (c) ability to expand its coordination number, and (d) propeller-like shape, would play a pivotal role in the stabilization of NDI radical ions and generation of stable highly electron-deficient NDI species. On the basis of these attributes, we designed the bis(phosphonium)-functionalized NDI $\mathbf{1a}^{2+}$ (Figure 2b). Calculations revealed a P···O distance of 2.814 Å, which is 0.636 Å smaller than the sum of the van der Waals radii of the P and O atoms (Figure 2c).[21] Therefore, it is clear from the optimized structure of $\mathbf{1a}^{2+}$ that P···O nonbonded interaction and the hypervalency should add to the thermodynamic stability and that the propeller-like shape of the phosphonium group should provide kinetic stability (Figure 2d). Natural bond orbital (NBO) calculations further validated this interaction in $\mathbf{1a}^{2+}$ as a donor–acceptor $n_O \rightarrow \sigma^*_{P-C}$ orbital interaction (Figure 2e).[22] Computational studies on the one-electron-reduced radical cation $\mathbf{1a}^{\bullet+}$ revealed a stronger P···O interaction (2.755 Å) resulting from the greater charge density on the peripheral imide O atoms in the $NDI^{\bullet-}$ core.

Toward the synthesis we followed phosphine coupling protocols with **NDI-(Br)$_2$**[23] using Pd catalysts. After several unsuccessful attempts, we performed an S_NAr reaction of **NDI-(Br)$_2$** with triphenylphosphine in various solvents. A reaction in the presence of a mild base in benzonitrile led to an air- and light-stable dark-green solution. Gratifyingly, this solution was found to be stable toward column chromatography, and a dark-green free-flowing solid could be isolated in excellent yield (~90%) (Figure 3a). Interestingly, the green solution, which remained silent to ^{1}H NMR, turned out to be the in situ-generated $\mathbf{1a}^{\bullet+}$, and its paramagnetic nature was confirmed by electron paramagnetic resonance (EPR) and UV–vis spectroscopy (vide infra). As envisaged, addition of the oxidant $NOBF_4$ to $\mathbf{1a}^{\bullet+}$ yielded a pale-yellow solution of $\mathbf{1a}^{2+}$, which was also stable toward air, light, and chromatography. $\mathbf{1a}^{2+}$ was characterized in detail by ^{1}H, ^{13}C, and ^{31}P NMR spectroscopy and other analytical techniques. Similarly, stable $\mathbf{1b}^{2+}$ and $\mathbf{1b}^{\bullet+}$ were isolated and characterized (see the Supporting Information). As shown in Figure 3b,c, the purities of $\mathbf{1a}^{\bullet+}$ and $\mathbf{1a}^{2+}$ could be easily verified by thin-layer chromatography (TLC), driven by their unprecedented stability.

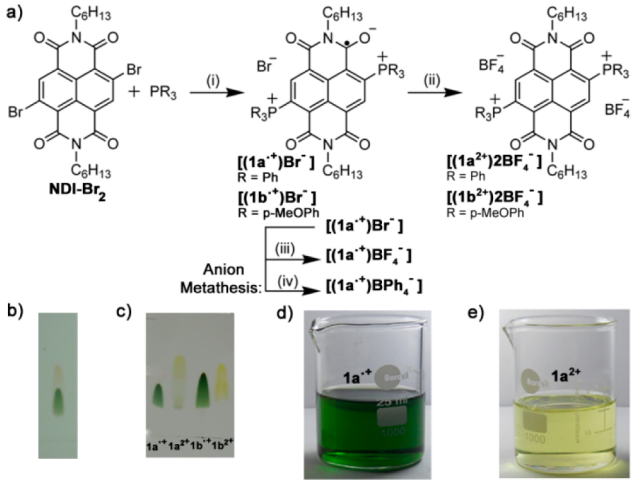

Figure 3. (a) Synthesis of $[(\mathbf{1a}^{\bullet+})Br^-]$, $[(\mathbf{1b}^{\bullet+})Br^-]$, $[(\mathbf{1a}^{2+})2BF_4^-]$, and $[(\mathbf{1b}^{2+})2BF_4^-]$. Reagents and conditions: (i) Et_3N, PhCN, 100 °C, 2 h, 90–93%; (ii) $NOBF_4$, $CHCl_3$, RT, 30 min, 70%; (iii) $NaBF_4$, MeOH/H_2O (7:3), RT, 30 min, 60%; (iv) $NaBPh_4$, MeOH, RT, 30 min, 60%. (b) TLC of a mixture of $\mathbf{1a}^{\bullet+}$ and $\mathbf{1a}^{2+}$. (c) TLC of the purified systems. (d, e) Chloroform solutions of remarkably stable (d) $\mathbf{1a}^{\bullet+}$ and (e) $\mathbf{1a}^{2+}$ in open air and laboratory light.

The solutions of $\mathbf{1a}^{\bullet+}$ and $\mathbf{1a}^{2+}$ showed extraordinary stability toward ambient air and light (Figure 3d,e). We studied the stability of $\mathbf{1a}^{\bullet+}$ for a period of 8 days in different solvents and also assessed the effect of concentration and the presence of water in these solvents under ambient conditions (Figure S1a–c in the Supporting Information). The amount of $\mathbf{1a}^{\bullet+}$ after 8 days remained unchanged in 0.4 mM MeCN and also in MeCN containing 5% water. Under similar conditions in MeOH, a 5–7% decrease in the amount of $\mathbf{1a}^{\bullet+}$ was observed, while in 0.4 mM $CHCl_3$ no significant change in the amount of $\mathbf{1a}^{\bullet+}$ was seen. $\mathbf{1a}^{\bullet+}$ in 0.4 mM and 5×10^{-5} M solutions in *N*,*N*-dimethylformamide (DMF) showed decreases of 9% and 35%, respectively. The decrease in the amount of $\mathbf{1a}^{\bullet+}$ in DMF was due to its slow conversion into the direduced species. The remarkable stability of the radical ion, particularly in MeCN and MeOH, allowed facile anion metathesis under ambient conditions.

Electrochemical Studies: Evaluation of Electron Deficiency. We evaluated the reduction potentials of $\mathbf{1a}^{2+}$ and $\mathbf{1b}^{2+}$ by applying cyclic voltammetry (CV) (Figure 4) and differential pulse voltammetry (DPV) (Figure S2 in the Supporting Information). To have a meaningful estimation, we compared our results with those for synthesized **NDI-(CN)$_2$** and freshly recrystallized tetracyanoquinodimethane (**TCNQ**) under similar experimental conditions. The CV studies demonstrated two reversible reduction peaks for $\mathbf{1a}^{2+}$ (−0.199 and −0.679 V vs Fc/Fc^+), $\mathbf{1b}^{2+}$ (−0.255 and −0.737 V vs Fc/Fc^+), **NDI-(CN)$_2$** (−0.570 and −1.111 V vs Fc/Fc^+), and **TCNQ** (−0.262 and −0.830 V vs Fc/Fc^+), corresponding to a sequential two-step ET process. This corresponds to a LUMO energy of −4.90 eV for $\mathbf{1a}^{2+}$ on the basis of E_{LUMO} = 5.1 eV for Fc against vacuum.[25] This is significantly lower than that for the super-π-acid **NDI-(EtSO$_2$)$_4$** (−4.74) and even that for **TCNQ**

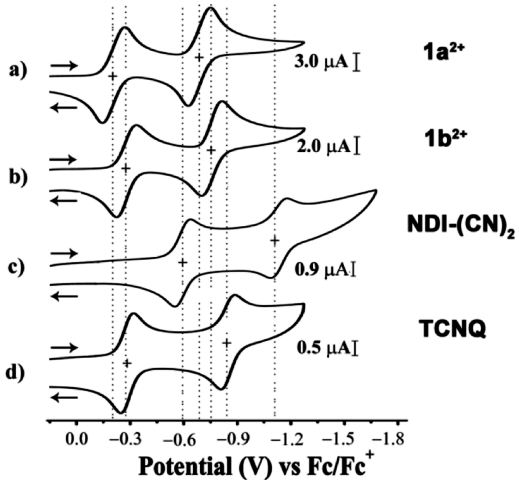

Figure 4. Cyclic voltammograms of (a) $\mathbf{1a}^{2+}$, (b) $\mathbf{1b}^{2+}$, (c) **NDI-(CN)$_2$**, and (d) **TCNQ**.[24] Conditions: 5×10^{-4} M in CH_2Cl_2; reference electrode, Ag/AgCl; working and auxiliary electrodes, Pt with 0.1 M Bu_4NPF_6 and ferrocene/ferrocenium (Fc/Fc^+); 298 K; scan rate, 200 mV/s.

dx.doi.org/10.1021/ja504903j | J. Am. Chem. Soc. 2014, 136, 12004–12010

(−4.84 eV), one of the most electron-deficient moieties known (Table S1 in the Supporting Information). Therefore, $\mathbf{1a}^{2+}$ is clearly ultra-electron-deficient. We also performed CV studies with a saturated calomel electrode (SCE) in MeCN to compare with the oxygen reduction potential ($E_{1/2}$ = +0.57 V vs SCE), a scale that can assess thermodynamic utility of electron-deficient systems under ambient conditions. $\mathbf{1a}^{2+}$ showed the first reduction potential at +0.172 V vs SCE, the closest achieved with any NDI moiety to date (Table S2 in the Supporting Information). Furthermore, $\mathbf{1b}^{2+}$ with the donor −OMe groups showed a distinct cathodic shift in the reduction potentials compared with $\mathbf{1a}^{2+}$. This confirmed the existence of electronic communication between the phosphonium and the NDI moieties. The LUMO level determined by DFT calculations[26] was in agreement with these results (Figure S3 in the Supporting Information).

X-ray Crystallographic Studies of $\mathbf{1a}^{2+}$. Next, we sought to grow single crystals of $\mathbf{1a}^{2+}$ in order to gain insight into the electronic, geometric, and stabilization effects of the phosphonium group on the NDI moiety. Gratifyingly, oxidation of $[(\mathbf{1a}^{\bullet+})\mathrm{Br}^-]$ with $NOBF_4$ and crystallization of the purified product led to air- and light-stable single crystals of $[(\mathbf{1a}^{2+})\text{-}2BF_4^-]$ (Figure S4 in the Supporting Information). It is noteworthy that all of the steps leading to the single crystals could be performed under ambient conditions.[27a]

The crystal structure revealed a distance of 2.776 Å from the P atoms of the phosphonium groups to the adjacent O atoms of the NDI imide groups (Figure 5a,b). This is significantly smaller than the sum of the van der Waals radii of the P and O atoms (ca. 3.45 Å)[21] but longer than the covalent P−O bond (1.689 Å)[28a] found in the phosphoranes. This corroborates an intramolecular O lone pair → P^+ interaction at the P center.[28b] On the basis of the bond angles around the P atom and the expansion of the P coordination number, the geometry was termed as a [4 + 1] monocapped tetrahedral geometry. Such pentacoordinated phosphonium ions have been found in aromatic chelates with pendant donor amino groups.[29] The phosphonium groups adopt a propeller-like arrangement.[30]

Furthermore, $\mathbf{1a}^{2+}$ shows the first direct evidence of interactions between the naphthalene unit of the NDI moiety and the anions. Notably, there is only very limited crystallographic evidence[9c] of anion−π interactions[31] with the NDI moiety. The structures known to date show interactions of the anions with the imide region of the NDI moiety. In $\mathbf{1a}^{2+}$, the two BF_4^- anions rest exactly on the top and bottom of the naphthalene π unit with the B atom at the center of the naphthalene ring (Figure 5c,d). The F···Ct (Ct = centroid of the naphthalene ring) distances range from 2.993 to 3.664 Å, and the closest point of separation between the NDI units is 6.7 Å. Interestingly, the BF_4^-−π interaction extends to form an infinite supramolecular array utilizing multiple C−H···F H-bonds involving the F atoms and the C−H bonds of the phenyl rings and the alkyl chains. The strong anion−π interactions corroborate the large electron deficiency of the naphthalene rings, in line with the electrostatic surface potential of $\mathbf{1a}^{2+}$ (Figure S5 in the Supporting Information). Therefore, the nonbonded P···O contact, propeller-like arrangement of the phosphonium group, and the anion−π interactions bestow remarkable thermodynamic and kinetic stability to $\mathbf{1a}^{2+}$.

Spectroscopic Studies. $\mathbf{1a}^{2+}$ and $\mathbf{1b}^{2+}$ showed strong UV absorption bands at 394 and 416 nm in chloroform due to the π−π^* transitions, which are significantly red-shifted by 36 and 38 nm compared with those of the bare NDI moiety, validating the stabilization of the LUMO orbital. $\mathbf{1a}^{2+}$ and $\mathbf{1b}^{2+}$ in the presence of a mild reducing agent such as TBACN readily embarked on a single ET reaction even in chloroform to form the dark-green colored $\mathbf{1a}^{\bullet+}$ and $\mathbf{1b}^{\bullet+}$, respectively. The uncluttered nature of the ET reaction and the presence of clear isosbestic points highlight the high stability of $\mathbf{1a}^{\bullet+}$ and $\mathbf{1b}^{\bullet+}$ (Figure 6a and Figure S6a in the Supporting Information).

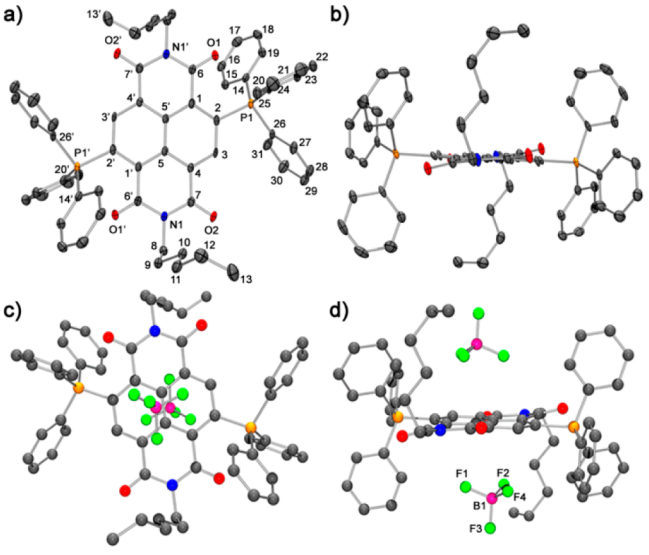

Figure 5. Crystal structure of $[(\mathbf{1a}^{2+})2BF_4^-]$. (a) Top- and (b) side-view ORTEP representations. Anions and H atoms have been removed for clarity. Thermal ellipsoids are shown at 50% probability. (c) Top- and (d) side-view POV-Ray depictions of the anion−π interactions. Selected bond lengths (Å): C1−C2 1.395(3), C2−C3 1.415(3), C3−C4 1.370(4), C1−C5′ 1.401(4), C4−C5 1.405(3), C5−C5′ 1.407(5), C6−O1 1.217(3), C7−O2 1.211(3), N1′−C6 1.385(3), N1′−C7′ 1.396(3), C2−P1 1.814(3), B···C5 3.528, B···C5′ 3.653, F1···Ct1 2.995, F2···Ct1 3.685, F4···Ct2 3.031. Selected bond angles (deg): C2−P1−C14 110.69(12), C2−P1−C20 109.58(12), C2−P1−C26 106.13(12). Selected torsion angles (deg): O1−C6−C1−C2 10.7(4), O2−C7−C4−C3 7.0(4).

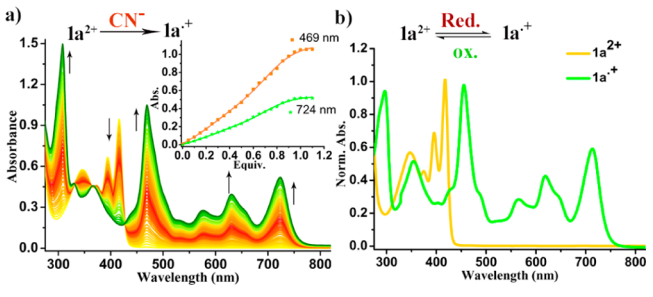

Figure 6. (a) UV−vis spectra depicting the gradual transformation of $\mathbf{1a}^{2+}$ to $\mathbf{1a}^{\bullet+}$ due to CN^--induced ET in $CHCl_3$ ($[\mathbf{1a}^{2+}] = 5 \times 10^{-5}$ M). Inset: CN^- dependence of the formation of $\mathbf{1a}^{\bullet+}$. (b) Electrochemical generation of $\mathbf{1a}^{\bullet+}$ from $\mathbf{1a}^{2+}$.

It is important to note that ET reactions of NDI have been limited only to polar solvents (dimethyl sulfoxide, DMF, etc.) and that in general radical ion formation in nonpolar solvents is extremely rare. The complete conversion of $\mathbf{1a}^{2+}/\mathbf{1b}^{2+}$ to $\mathbf{1a}^{\bullet+}/\mathbf{1b}^{\bullet+}$ could be confirmed by the complete disappearance of the intense bands at 394 and 416 nm. The purified radical ions isolated after the in situ synthesis and after addition of the dedicated reducing agents or after anion metathesis exhibited

dx.doi.org/10.1021/ja504903j | J. Am. Chem. Soc. 2014, 136, 12004−12010

the same molar absorptivity (Figure S6b in the Supporting Information).

The signature absorption peaks at 308, 469, 572, 630, and 724 nm perfectly matched with those of electrochemically generated $\mathbf{1a}^{\bullet+}$ (Figure 6b and Figure S7 in the Supporting Information). Addition of an additional equivalent of TBACN resulted in the formation of the direduced neutral NDI species (Figure S8 in the Supporting Information).

It should be noted that the main absorption characteristics of $\mathbf{1a}^{\bullet+}$ closely resemble those of $NDI^{\bullet-}$, with the most intense absorption band appearing around 470 nm. Therefore, $\mathbf{1a}^{\bullet+}$ maintains the predominant optoelectronic characteristics of $NDI^{\bullet-}$ due to similar $D_0 \rightarrow D_n$ transitions. It is also important to note that $NDI^{\bullet+}$ recently synthesized in our group by chemical oxidation exhibited completely different absorption characteristics, with the most intense absorption band appearing at 874 nm.[18a]

IR spectroscopy exhibited a large shift in the symmetric and asymmetric stretching frequencies of the imide carbonyl from 1710 and 1657 cm^{-1} in $\mathbf{1a}^{2+}$ to 1651 and 1606 cm^{-1} in $\mathbf{1a}^{\bullet+}$, confirming the greater single-bond character of the carbonyl groups (Figure S9 in theSupporting Information). The paramagnetic nature of $\mathbf{1a}^{\bullet+}$ was also confirmed as the solution remained silent to NMR and an EPR peak with $g = 2.004$ was observed (Figures S10 and S11 in the Supporting Information).

Anion Metathesis and Crystallographic Studies of $\mathbf{1a}^{\bullet+}$. Further, we set out to crystallize $[(\mathbf{1a}^{\bullet+})Br^-]$ to understand the bonding environment and origin of stabilization of the radical ion. Dark-green crystals appeared under ambient conditions, but they did not diffract X-rays. To enhance the crystallinity, we performed metathesis of the bromide salt, which was greatly facilitated by the high stability of $\mathbf{1a}^{\bullet+}$ in MeOH/MeCN. With sodium tetraphenylborate as the anion, highly stable, good-quality single crystals could be grown from a solution of toluene and dichloromethane (Figure S4 in the Supporting Information). It is noteworthy that all of the steps leading to crystallization could be performed under ambient conditions and did not require any air-protective safeguards or ultralow-temperature refrigeration, a necessity for crystallization of radical ions.

The crystal data for $[(\mathbf{1a}^{\bullet+})BPh_4^-]$ confirmed the molecular composition of $[C_{62}H_{58}N_2O_4P_2]^+[C_{24}H_{20}B]^-$.[27b] Therefore, $[(\mathbf{1a}^{\bullet+})BPh_4^-]$ can be represented as $[NDI^{\bullet-}-(Ph_3P^+)_2]BPh_4^-$, since the positive charges of the phosphonium groups are counterbalanced by the charge associated with $NDI^{\bullet-}$ and the tetraphenylborate anion. The NDI ring in $\mathbf{1a}^{\bullet+}$ compared with that in $\mathbf{1a}^{2+}$ revealed significant bond lengthening in the transverse (C1−C2 and C3−C4), annular (C5−C5′), and imide bonds (N1′−C6′ and N1′−C7′) along with small changes in the P−C bond lengths, bond angles, and tetrahedral geometry of the P atoms (Figure 7a,b). The imide carbonyls adjacent to the phosphonium groups in $\mathbf{1a}^{\bullet+}$ show a bond length increase of 0.017 Å (cf. $\mathbf{1a}^{2+}$). Importantly, $\mathbf{1a}^{\bullet+}$ exhibits a stronger $O_{(RA)} \rightarrow P^+$ donor−acceptor interaction (compared with $\mathbf{1a}^{2+}$), with a decrease of 0.057 Å in the O···P distance, while maintaining the [4 + 1] monocapped tetrahedral geometry. This is evidently due to the enhanced charge transfer through the O atoms propelled by the extra electron in $\mathbf{1a}^{\bullet+}$. The BPh_4^- anion is positioned between two NDI radical ions, forming anion−π interactions as well as bestowing kinetic protection (Figure 7c). Therefore, the O···P interaction, hypervalency, and combined steric encumbrance through the propeller-shaped phosphonium group and the bulky anion

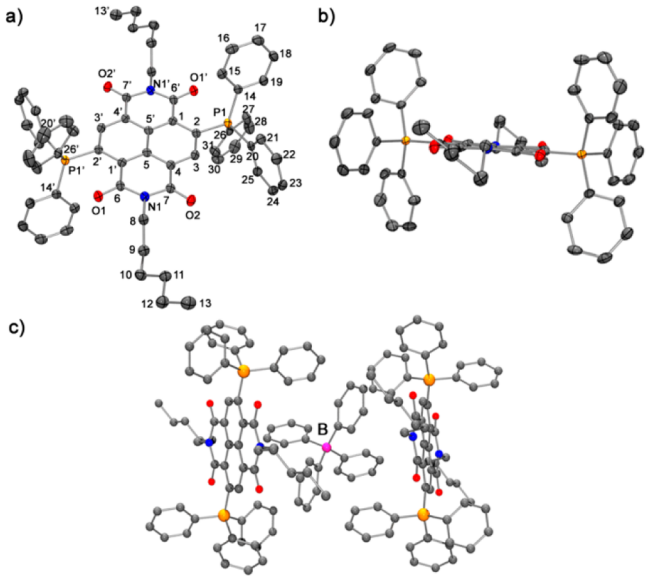

Figure 7. Crystal structure of $[(\mathbf{1a}^{\bullet+})BPh_4^-]$. (a) Top- and (b) side-view ORTEP representations. BPh_4^- and H atoms have been removed for clarity. Thermal ellipsoids are shown at 50% probability. (c) POV-Ray representation of the interaction of BPh_4^- with the NDI moiety. Selected bond lengths (Å): C1−C2 1.428(3), C2−C3 1.390(3), C3−C4 1.391(3), C1−C5′ 1.408(3), C4−C5 1.409(3), C5−C5′ 1.421(4), C6−O1 1.233(3), C7−O2 1.225(3), N1−C6 1.396(3), N1−C7 1.400(3), C2−P1 1.807(2). Selected bond angles (deg): C2−P1−C14 110.21(10), C2−P1−C20 105.00(10), C2−P1−C26 113.23(11). Selected torsion angles (deg): O1−C12−C1−C2 3.4(3), O2−C13−C4−C3 2.4(3).

result in the extraordinary stability of this radical ion. It should be noted that this is the first structural insight into a discrete NDI radical ion.

Theoretical Studies. The theoretically calculated geometry of the phosphonium groups and the bond alterations in $\mathbf{1a}^{2+}$ and $\mathbf{1a}^{\bullet+}$ were in line with the X-ray crystallographic results (Table S3 in the Supporting Information). Computational studies predicted that the intramolecular nonbonded O lone pair → P^+ interaction and the ability of the phosphonium group to increase its coordination number in $\mathbf{1a}^{2+}$ and $\mathbf{1a}^{\bullet+}$ should be the key thermodynamic stabilizing elements. Along with this, the propeller-like shape of the phosphonium group should provide kinetic protection. NBO calculations on $\mathbf{1a}^{2+}$ corroborated the P···O contact to be a donor−acceptor-type $n_O \rightarrow \sigma^*_{P-C}$ orbital interaction (Figure 2e). Furthermore, atoms in molecules (AIM) calculations[32] established the presence of a bond path between the P and O atoms with an electron density $\rho(r)$ of 1.84×10^{-2} e $bohr^{-3}$ at the bond critical points (BCPs) (Figure 8).

Charge and spin density calculations on $\mathbf{1a}^{\bullet+}$ and a comparison with the radical anion form of **NDI** (**NDI-R**) provided further credence to the above findings (Tables S4−S6 in the Supporting Information). Spin density calculations on $\mathbf{1a}^{\bullet+}$ clearly demonstrated that the spin is mostly delocalized over the core of the naphthalene ring (C1, C2, C4, C5, C6, and C8). The C atoms C3 and C7 were found to have small residual negative spins, while the spins on the two O atoms interact with the vacant orbitals of the P atom (Figure 9a). In sharp contrast, **NDI-R** has considerable spin delocalized over the peripheral imide rings and the substitutable C atoms of the naphthalene ring, rendering **NDI-R** unstable (Figure 9b). In

dx.doi.org/10.1021/ja504903j | J. Am. Chem. Soc. 2014, 136, 12004−12010

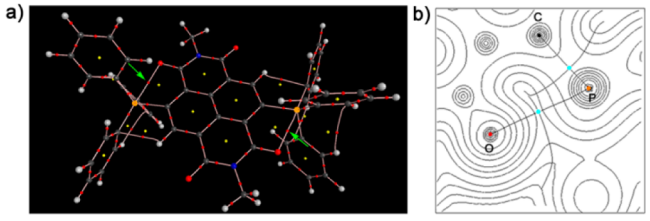

Figure 8. Atoms in molecules (AIM) calculations on $\mathbf{1a}^{2+}$. (a) 3D plot showing bond critical points (BCPs) (red) and ring critical points (RCPs) (yellow). The green arrows indicate the BCPs between P and O atoms. (b) AIM electron density map with relevant bond paths and BCPs.

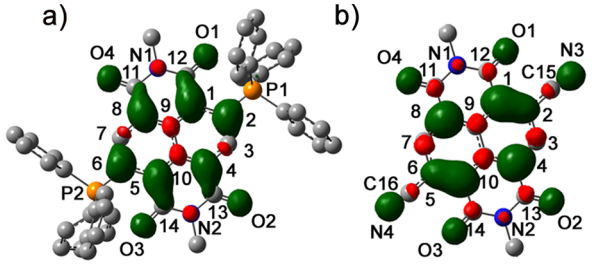

Figure 9. Spin density distributions of (a) $\mathbf{1a}^{\bullet+}$ and (b) **NDI-R**.

addition, Mulliken charge distribution analysis clearly exhibited an enhancement of charge distribution over the imide oxygen atoms in $\mathbf{1a}^{\bullet+}$ compared with $\mathbf{1a}^{2+}$ (Table S6 in the Supporting Information), substantiating a greater O → P^+ interaction in $\mathbf{1a}^{\bullet+}$ in line with the single-crystal data. Therefore, apart from imparting thermodynamic and kinetic stabilization, the phosphonium group can also effectively shield the spin from the reactive centers of the NDI moiety.

CONCLUSION

We have established new elements of stabilization utilizing the multifaceted features of the phosphonium group, enabling the isolation of the first NDI-based radical ion and ultra-electron-deficient NDI systems, which hitherto have remained elusive under open-air conditions. One of the most striking findings is the attainment of the extraordinary stability leading to their synthesis, purification, and crystallization, all under ambient conditions. To the best of our knowledge, this is the first instance of a radical ion that exhibits endurance toward silica-gel chromatography. This is highly appealing from the point of view of synthetic radical/radical ion chemistry. This new design paradigm also accomplishes the lowest LUMO level recorded to date for any NDI molecule, surpassing that of **TCNQ**, while maintaining excellent stability. The first structural evidence of the NDI radical ion highlighted important insights into the bond alterations due to the unpaired electron. In addition, the crystal structure of the ultra-electron-deficient system provided direct evidence of interactions between the anions and the naphthalene core of the NDI moiety. The facile ET even in nonpolar solvents highly modulates the optical properties of the NDI radical ion, providing attractive prospects toward switchable panchromatic materials.[33] In line with the huge interest in isolating P-based stable radical ions,[34] this new concept paves the way for the utilization of the various donor–acceptor n → σ^* and n → π^* interactions[35] toward new spin-based research. Also, from the chemical biology perspective, the ability of the lipophilic phosphonium group to selectively localize in the mitochondria of the cell might afford new spin-based diagnostic tools.[36]

ASSOCIATED CONTENT

Supporting Information

Details of the synthesis and analytical characterization of the molecules by NMR, MALDI-TOF MS, EPR, and UV–vis spectroscopy; CV and DPV studies; X-ray crystallography (CIF); theoretical studies; and coordinates of the geometry-optimized structures (TXT). This material is available free of charge via the Internet at http://pubs.acs.org.

AUTHOR INFORMATION

Corresponding Author

m_pritam@mail.jnu.ac.in

Author Contributions

[§]S.K. and M.R.A. contributed equally.

Author Contributions

[‖]G.H. performed X-ray crystallography.

Notes

The authors declare no competing financial interest.

ACKNOWLEDGMENTS

We thank the DBT-BUILDER and DST-PURSE Projects for financial assistance and DST-FIST for funding of the instrumentation facilities. S.K. and M.R.A. thank UGC and CSIR for their research fellowships. We are thankful to Dr. R. Banerjee and Mr. C. Dey (NCL Pune) for their numerous attempts to collect the single-crystal X-ray data for the radical ions with Br^- and BF_4^- anions. We thank AIRF (JNU, New Delhi) for the instrumentation facilities and Dr. R. P. Pant (NPL, New Delhi) for the EPR facility.

REFERENCES

(1) (a) Morita, Y.; Nishida, S. *Stable Radicals: Fundamental and Applied Aspects of Odd-Electron Compounds*; Hicks, R., Ed.; Wiley-Blackwell: New York, 2010. (b) *Magnetism: Molecules to Materials II*; Miller, J. S., Drillon, M. Eds.; Wiley-VCH: Weinheim, Germany, 2001. (c) Kahn, O. *Molecular Magnetism*; VCH: New York, 1993.

(2) (a) Haddon, R. C. *Nature* **1975**, *256*, 394. (b) Torrent, M. M.; Crivillers, N.; Rovira, C.; Veciana, J. *Chem. Rev.* **2012**, *112*, 2506–2527. (c) Morita, Y.; Suzuki, S.; Sato, K.; Takui, T. *Nat. Chem.* **2011**, *3*, 197. (d) Power, P. P. *Chem. Rev.* **2003**, *103*, 789–810.

(3) (a) Klauk, H. *Organic Electronics: Materials, Manufacturing and Applications*; Wiley-VCH: Weinheim, Germany, 2006. (b) Nakanishi, T. *Supramolecular Soft Matter: Applications in Materials and Organic Electronics*; Wiley-Blackwell: Hoboken, NJ, 2011.

(4) (a) Smith, M. B.; March, J. *Advanced Organic Chemistry: Reactions, Mechanisms and Structure*, 6th ed.; John Wiley and Sons: Hoboken, NJ, 2007. (b) Minkin, V. I.; Minyaev, R. M. *Chem. Rev.* **2001**, *101*, 1247.

(5) (a) Baumgartner, T. *Acc. Chem. Res.* **2014**, *47*, 1613. (b) He, X.; Lin, J.-B.; Kan, W. H.; Baumgartner, T. *Angew. Chem., Int. Ed.* **2013**, *52*, 8990. (c) Ren, Y.; Kan, W. H.; Thangadurai, V.; Baumgartner, T. *Angew. Chem., Int. Ed.* **2012**, *51*, 3964.

(6) (a) Hudnall, T. W.; Chiu, C.-W.; Gabbaï, F. P. *Acc. Chem. Res.* **2009**, *42*, 388. (b) Hudnall, T. W.; Kim, Y.-M.; Bebbington, M. W. P.; Bourissou, D.; Gabbaï, F. P. *J. Am. Chem. Soc.* **2008**, *130*, 10890. (c) Kim, Y.; Hudnall, T. W.; Bouhadir, G.; Bourissou, D.; Gabbaï, F. P. *Chem. Commun.* **2009**, 3729. (d) Kim, Y.; Huh, H.-S.; Lee, M. H.; Lenov, I. L.; Zhao, H.; Gabbaï, F. P. *Chem.—Eur. J.* **2011**, *17*, 2057.

(7) Ichikawa, T.; Yoshio, M.; Hamasaki, A.; Taguchi, S.; Liu, F.; Zeng, X.-B.; Ungar, G.; Ohno, H.; Kato, T. *J. Am. Chem. Soc.* **2012**, *134*, 2634.

(8) (a) Wade, C. R.; Li, M.; Dincă, M. *Angew. Chem., Int. Ed.* **2013**, *52*, 13377. (b) Takai, A.; Yasuda, T.; Ishizuka, T.; Kojima, T.; Takeuchi, M. *Angew. Chem., Int. Ed.* **2013**, *52*, 9167. (c) Avinash, M. B.; Govindaraju, T. *Adv. Mater.* **2012**, *24*, 3905. (d) Cougnon, F. B. L.; Jenkins, N. A.; Pantos, G. D.; Sanders, J. K. M. *Angew. Chem., Int. Ed.* **2012**, *51*, 1443. (e) Gunderson, V. L.; Smeigh, A. L.; Kim, C. H.; Co, D. T.; Wasielewski, M. R. *J. Am. Chem. Soc.* **2012**, *134*, 4363. (f) Tu, S.; Kim, S. H.; Joseph, J.; Modarelli, D. A.; Parquette, J. R. *J. Am. Chem. Soc.* **2011**, *133*, 19125. (g) Röger, C.; Miloslavina, Y.; Brunner, D.; Holzwarth, A. R.; Würthner, F. *J. Am. Chem. Soc.* **2008**, *130*, 5929. (h) Reczek, J. J.; Villazor, K. R.; Lynch, V.; Swager, T. M.; Iverson, B. L. *J. Am. Chem. Soc.* **2006**, *128*, 7995.

(9) (a) Gorteau, V.; Bollot, G.; Mareda, J.; Velasco, A. P.; Matile, S. *J. Am. Chem. Soc.* **2006**, *128*, 14788. (b) Dawson, R. E.; Hennig, A.; Weimann, D. P.; Emery, D.; Ravikumar, V.; Montenegro, J.; Takeuchi, T.; Mareda, M. J.; Schalley, C. A.; Matile, S. *Nat. Chem.* **2010**, *2*, 533. (c) Guha, S.; Goodson, F. S.; Clark, R. J.; Saha, S. *CrystEngComm* **2012**, *14*, 1213. (d) Sisson, A. L.; Sakai, N.; Banerji, N.; Fürstenberg, A.; Vauthey, E.; Matile, S. *Angew. Chem., Int. Ed.* **2008**, *47*, 3727.

(10) (a) Domoto, Y.; Orentas, E.; Beuchat, C.; Emery, D.; Mareda, J.; Sakai, N.; Matile, S. *Angew. Chem., Int. Ed.* **2013**, *52*, 9940. (b) Zhao, Y.; Beuchat, C.; Domoto, Y.; Gajewy, J.; Wilson, A.; Mareda, J.; Sakai, N.; Matile, S. *J. Am. Chem. Soc.* **2014**, *136*, 2101.

(11) (a) Ajayakumar, M. R.; Mukhopadhyay, P. *Chem. Commun.* **2009**, 3702. (b) Ajayakumar, M. R.; Yadav, S.; Ghosh, S.; Mukhopadhyay, P. *Org. Lett.* **2010**, *12*, 2646. (c) Ajayakumar, M. R.; Hundal, G.; Mukhopadhyay, P. *Chem. Commun.* **2013**, *49*, 7684.

(12) Guha, S.; Saha, S. *J. Am. Chem. Soc.* **2010**, *132*, 17674.

(13) (a) Holman, G. G.; Foote, M. Z.; Smith, A. R.; Johnson, K. A.; Iverson, B. L. *Nat. Chem.* **2011**, *3*, 875. (b) Chu, Y.; Hoffman, D. W.; Iverson, B. L. *J. Am. Chem. Soc.* **2009**, *131*, 3499. (c) Smith, A. R.; Iverson, B. L. *J. Am. Chem. Soc.* **2013**, *135*, 12783.

(14) (a) Katz, H. E.; Lovinger, A. J.; Kloc, C.; Siegrist, T.; Li, W.; Lin, Y.-Y.; Dodabalapur, A. *Nature* **2000**, *404*, 478−481. (b) Jones, B. A.; Facchetti, A.; Wasielewski, M. R.; Marks, T. J. *J. Am. Chem. Soc.* **2007**, *129*, 15259. (c) Chen, Z.; Zheng, Y.; Yan, H.; Facchetti, A. *J. Am. Chem. Soc.* **2009**, *131*, 8. (d) Zhang, F.; Hu, Y.; Schuettfort, T.; Di, C.-a.; Gao, X.; McNeill, C. R.; Thomsen, L.; Mannsfeld, S. C. B.; Yuan, W.; Sirringhaus, H.; Zhu, D. *J. Am. Chem. Soc.* **2013**, *135*, 2338. (e) Earmme, T.; Hwang, Y.-J.; Murari, N. M.; Subramaniyan, S.; Jenekhe, S. A. *J. Am. Chem. Soc.* **2013**, *135*, 14960.

(15) Nelsen, S. F. *J. Am. Chem. Soc.* **1967**, *89*, 5925.

(16) A *persistent* radical has a relatively long lifetime under the conditions where it is generated and eventually undergoes decomposition, whereas a *stable* radical can be isolated under ambient conditions and stored indefinitely without decomposition.

(17) Heywang, G.; Born, L.; Fitzky, H.-G.; Hassel, T.; Hocker, J.; Müller, H.-K.; Pittel, B.; Roth, S. *Angew. Chem., Int. Ed. Engl.* **1989**, *28*, 483.

(18) (a) Ajayakumar, M. R.; Asthana, D.; Mukhopadhyay, P. *Org. Lett.* **2012**, *14*, 4822. (b) Asthana, D.; Ajayakumar, M. R.; Pant, R. P.; Mukhopadhyay, P. *Chem. Commun.* **2012**, *48*, 6475.

(19) (a) Chang, J.; Ye, Q.; Huang, K.-W.; Zhang, J.; Chen, Z.-K.; Wu, J.; Chi, C. *Org. Lett.* **2012**, *14*, 2964. (b) Kivala, M.; Boudon, C.; Gisselbrecht, J.-P.; Enko, B.; Seiler, P.; Muller, I. B.; Langer, N.; Jarowski, P. D.; Gescheidt, G.; Diederich, F. *Chem.—Eur. J.* **2009**, *15*, 4111. (c) Jones, B. A.; Facchetti, A.; Wasielewski, M. R.; Marks, T. J. *J. Am. Chem. Soc.* **2007**, *129*, 15259. (d) Würthner, F. *Angew. Chem., Int. Ed.* **2001**, *40*, 1037.

(20) Míšek, J.; Jentzsch, A. V.; Sakurai, S.-i.; Emery, D.; Mareda, J.; Matile, S. *Angew. Chem., Int. Ed.* **2010**, *49*, 7680.

(21) Batsanov, S. S. *Inorg. Mater.* **2001**, *37*, 871.

(22) Glendening, E. D.; Badenhoop, J. K.; Reed, A. E.; Carpenter, J. E.; Bohmann, J. A.; Morales, C. M.; Landis, C. R.; Weinhold, F. *NBO 6.0*; Theoretical Chemistry Institute, University of Wisconsin: Madison, WI, 2013.

(23) Thalacker, C.; Röger, C.; Würthner, F. *J. Org. Chem.* **2006**, *71*, 8098.

(24) **NDI-$(CN)_2$** was freshly synthesized and **TCNQ** was recrystallized prior to use.

(25) Cardona, C. M.; Li, W.; Kaifer, A. E.; Stockdale, D.; Bazan, G. C. *Adv. Mater.* **2011**, *23*, 2367.

(26) For details of the B3LYP/6-31G+(d,p) and UB3LYP/6-31G +(d,p) DFT calculations, see the Supporting Information.

(27) CCDC 963831 ($\mathbf{1a}^{2+}$) and CCDC 963832 ($\mathbf{1a}^{\bullet+}$) contain the supplementary crystallographic data for this paper. These data can be obtained free of charge from The Cambridge Crystallographic Data Centre via www.ccdc.cam.ac.uk/data_request/cif. (a) Crystal data for $\mathbf{1a}^{2+}$: $C_{62}H_{58}N_2O_4P_2\cdot(BF_4)_2$, M = 1130.66, triclinic, $P\bar{1}$, a = 11.263(3) Å, b = 12.130(4) Å, c = 12.624(5) Å, α = 105.577(5)°, β = 101.089(3)°, γ = 110.247(5)°, V = 1479.0(9) Å^3, Z = 1, Mo Kα radiation (λ = 0.71073 Å), T = 100.0(2) K, μ = 0.146 mm^{-1}, F(000) = 588, crystal size 0.18 mm × 0.16 mm × 0.09 mm, Bruker APEX-II CCD diffractometer, 18 900 reflections, 5443 independent reflections (R_{int} = 0.0547) and 3626 observed reflections [$I \geq 2\sigma(I)$], 361 refined parameters, R = 0.0547, wR_2 = 0.1287. (b) Crystal data for $\mathbf{1a}^{\bullet+}$: $C_{62}H_{58}N_2O_4P_2\cdot C_{24}H_{20}B$, M = 1276.25, monoclinic, $C2/c$, a = 29.158(3) Å, b = 15.807(17) Å, c = 20.093(2) Å, α = 90°, β = 127.454(3)°, γ = 90°, V = 7351.7(13) Å^3, Z = 4, Mo Kα radiation (λ = 0.71073 Å), T = 100.0(2) K, μ = 0.146 mm^{-1}, F(000) = 2700, crystal size 0.18 mm × 0.16 mm × 0.10 mm, Bruker APEX-II CCD diffractometer, 25 987 reflections, 6977 independent reflections (R_{int} = 0.0621) and 4480 observed reflections [$I \geq 2\sigma(I)$], 429 refined parameters, R = 0.0542, wR_2 = 0.1239.

(28) (a) Allen, F. H.; Kennard, O.; Watson, D. G.; Brammer, L.; Orpen, A. G.; Taylor, R. *J. Chem. Soc., Perkin Trans. 2* **1987**, S1−S19. (b) O → P notation has been used as this interaction is longer than a typical single bond and has a charge-transfer character. See: Haaland, A. *Angew. Chem., Int. Ed. Engl.* **1989**, *28*, 992.

(29) For the [4 + 1] monocapped tetrahedral geometry, see: Chuit, C.; Corriu, R. J. P.; Manforte, P.; Reyé, C.; Declercq, J.-P.; Duborg, A. *Angew. Chem., Int. Ed. Engl.* **1993**, *32*, 1430.

(30) For the propeller-like arrangemnt of Ph rings, see: Braunschweig, H.; Dyakonov, V.; Engels, B.; Falk, Z.; Hörl, C.; Klein, J. H.; Kramer, T.; Kraus, H.; Krummenacher, I.; Lambert, C.; Walter, C. *Angew. Chem., Int. Ed.* **2013**, *52*, 12852.

(31) (a) Chifotides, H. T.; Dunbar, K. R. *Acc. Chem. Res.* **2013**, *46*, 894. (b) Ballester, P. *Acc. Chem. Res.* **2013**, *46*, 874. (c) Frontera, A.; Gamez, P.; Mascal, M.; Mooibroek, T. J.; Reedijk, J. *Angew. Chem., Int. Ed.* **2011**, *50*, 9564. (d) Salonen, L. M.; Ellermann, M.; Diederich, F. *Angew. Chem., Int. Ed.* **2011**, *50*, 4808.

(32) (a) Biegler-König, F.; Bader, R. F. W.; Tang, T. H. *J. Comput. Chem.* **1982**, *13*, 317. (b) Bader, R. F. W. *Atoms in Molecules: A Quantum Theory*; Clarendon Press: Oxford, U.K., 1990.

(33) Motiei, L.; Lahav, M.; Freeman, D.; van der Boom, M. E. *J. Am. Chem. Soc.* **2009**, *131*, 3468.

(34) (a) Pan, X.; Su, Y.; Chen, X.; Zhao, Y.; Li, Y.; Zuo, J.; Wang, X. *J. Am. Chem. Soc.* **2013**, *135*, 5561. (b) Back, O.; Donnadieu, B.; von Hopffgarten, M.; Klein, S.; Tonner, R.; Frenking, G.; Bertrand, G. *Chem. Sci.* **2011**, *2*, 858. (c) Back, O.; Donnadieu, B.; Parameswaran, P.; Frenking, G.; Bertrand, G. *Nat. Chem.* **2010**, *2*, 369.

(35) (a) Newberry, R. W.; Veller, B. V.; Guzei, I. A.; Raines, R. T. *J. Am. Chem. Soc.* **2013**, *135*, 7843. (b) Lin, T.-P.; Ke, I.-S.; Gabbaï, F. P. *Angew. Chem., Int. Ed.* **2012**, *51*, 4985. (c) Zhao, H.; Gabbaï, F. P. *Nat. Chem.* **2010**, *2*, 984.

(36) Rideout, D.; Bustamante, A.; Patel, J. *Int. J. Cancer* **1994**, *57*, 247.